Radar analysis of warm rain showers[1]

BY R. G. SEMONIN, E. A. MUELLER, G. E. STOUT and D. W. STAGGS, *Illinois State Water Survey, Urbana, Illinois*

(Manuscript received May 17, 1967)

ABSTRACT

Two X-band radar sets, an M-33 and a GPG-1, were operated routinely on the island of Hawaii during the period July 11 through August 28, 1965. The M-33 was located at the Cloud Physics Observatory on the Hilo Campus of the University of Hawaii. The data obtained from the PPI scope photography were used to determine preliminary climatological parameters associated with trade wind showers.

The relationship between echo frequency and total rainfall was examined and found to be remarkably good. Such an analysis is useful in the determination of rainfall amounts over the land and over the ocean in the vicinity of Hawaii where the raingage density is sparse.

The frequency of echoes of a given diameter as a function of range was tabulated according to whether the echo was observed over land or over water. It is apparent from these data that there was a greater frequency of echoes per unit area over land than over water. This is attributed to the breakup of organized lines or bands of showers as they moved inland. In addition, there is a distinct decrease of echo frequency with range. The observed decrease of echo frequency cannot be accounted for by range attenuation or atmospheric refraction.

The relationship between echo movement and the trade winds was studied. The results indicate that the radar echoes tend to move to the right of the wind direction with a slightly greater speed than the environmental wind.

Selected examples of radar photographs are presented which illustrate typical echo displays. In addition, the radar presentation of a mesosystem and the echoes associated with a Hawaiian thunderstorm are shown.

The GPG-1 radar was located at 2100 meters on the windward slope of Mauna Kea. Very little useful data were obtained from this location due to trapping gradients associated with the trade inversion. An example is shown where the propagation path was extended and the sensitivity reduced by refractive index gradients. The site was abandoned early in the project in favor of a more concentrated effort on the M-33 operations.

Introduction

In support of a concerted attack on the warm rain mechanism, two X-band radar sets were operated routinely on the island of Hawaii during the period July 11 through August 28, 1965. The cooperative project involved cloud physicists from the United States and Japan who collaborated to obtain measurements on the structure and chemical composition of trade wind showers.

There were three locations chosen as sites for the various radars, a balloon launching platform, and the field headquarters for the Japanese. The elevations for these sites were 56, 780, and 2100 meters above sea level. This report will be concerned with the M-33 radar operations at the 56 meter level, Cloud Physics Observatory (CPO), Hilo Campus, U. of Hawaii and the GPG-1 radar operations at the 2100 meter level on Mauna Kea. These locations are indicated in Fig. 1.

[1] Part of the "Warm Rain Project", the results of which were published in Tellus 19, 347–516.

Radar characteristics

M-33

The primary radar used for data collection was the tracking radar of an M-33 system supplied by the National Center for Atmospheric Research, (NCAR) Boulder, Colorado. This radar, shown in Fig. 2*a*, was located at the CPO. The radar was equipped with a step gain control, an antenna elevation control, and a

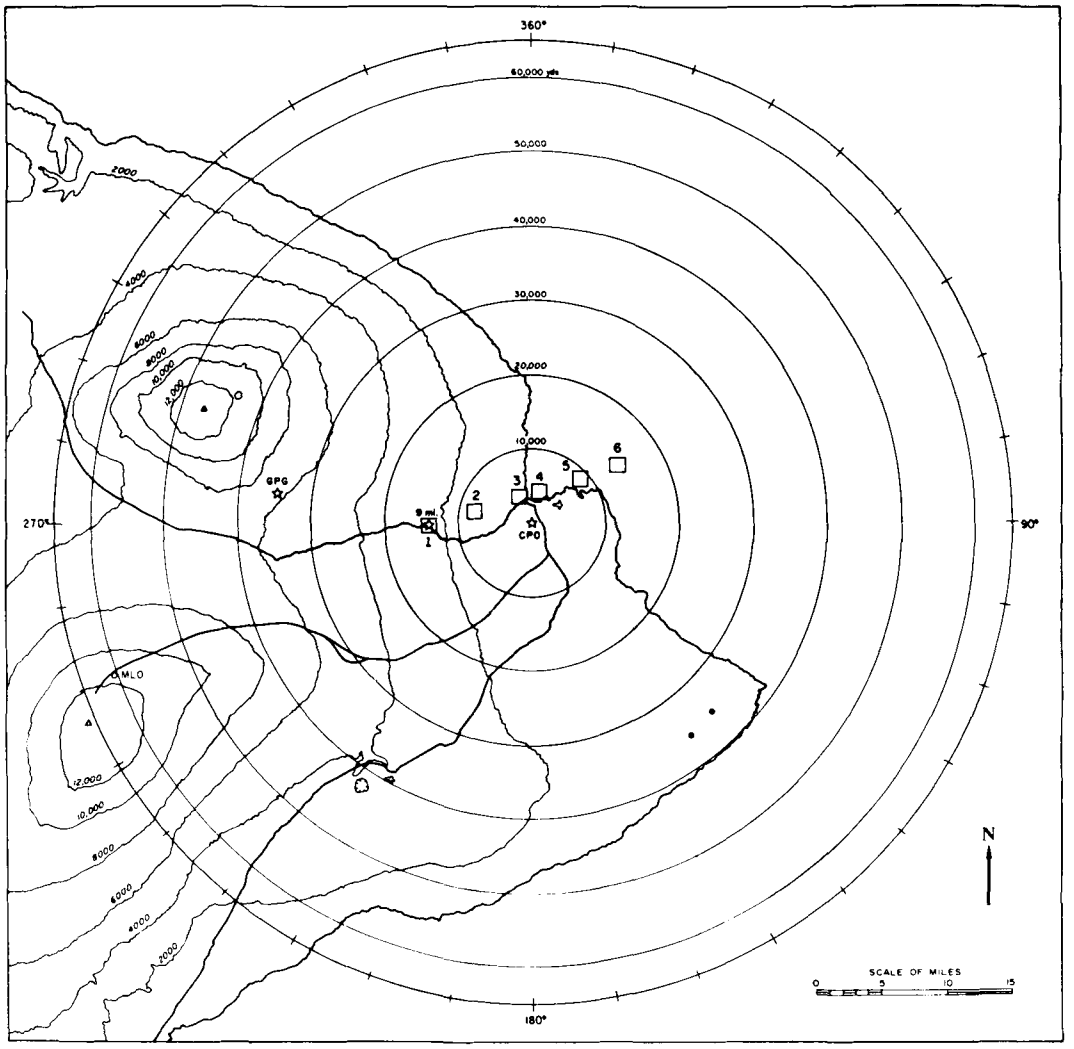

Fig. 1. Radar locations and the Japanese balloon launching site on the east side of the island of Hawaii.

camera. The step gain control provided for two modes of operation. In one mode the nominal difference in sensitivity of two adjacent steps was 4 db. In mode 2 the difference was about 8 db.

The antenna operating mode allowed the elevation angle to be programmed. There were 10 elevation angles plus two types of 0° (horizontal) operation incorporated into the antenna mode programmer. In one type of 0° operation (referred to as split-Z), the antenna was held at 0° through the eastern semicircle (ocean area) and was raised to about 4½° through the western semicircle (land area). This elevation angle in the western sector allowed the radar to look above the majority of the ground return from the mountain slopes. The technique proved valuable and most of the routine data were taken with this mode of operation. In addition to these changes in the antenna drive system, NCAR provided a modification of the range of the PPI scope and added range marks.

The M-33 was calibrated using a 10-inch diameter metallic sphere flown on a Jalbert wing on two occasions. These two calibrations, which agree to within 2 db were made on July 9 and on August 20, 1965. The two independent measures of overall performance using the

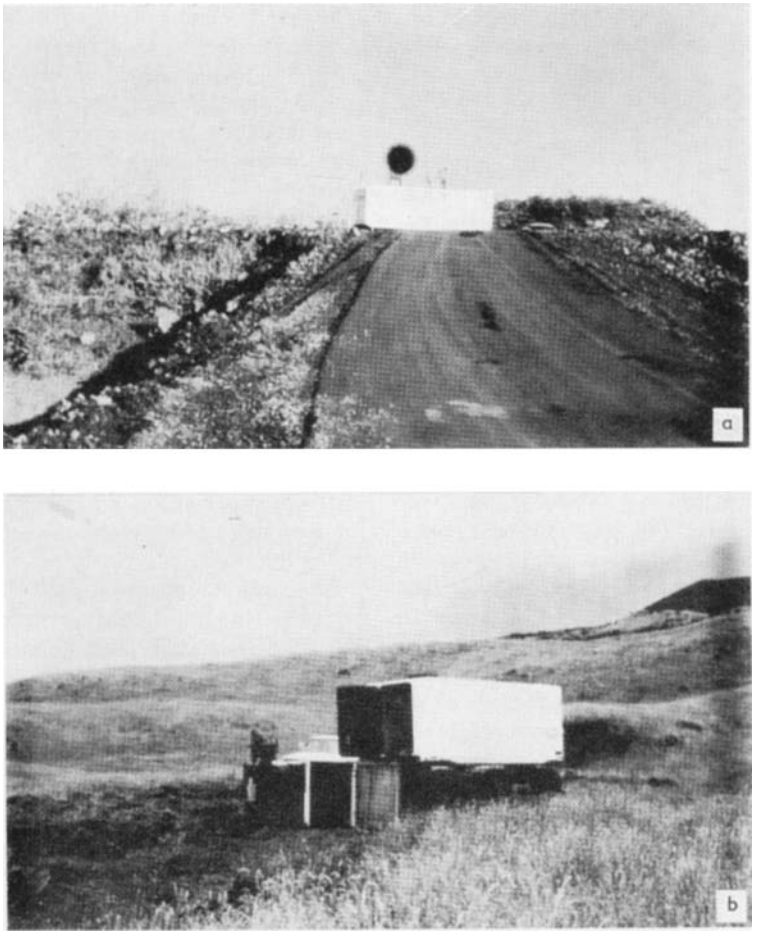

Fig. 2. The M-33, X-band tracking radar and the GPG-1, X-band radar on location. (*a*) M-33 at the Cloud Physics Observatory with the cloud camera on top of the van. (*b*) The GPG-1 and maintenance van at the 2100 meter level on Mauna Kea.

metallic spheres yielded values for antenna gain of 36 db and 38 db. Table 1 contains the measured characteristics and nominal characteristics of the radar. The transmitter power was always operated at lower than rated values. Receiver sensitivities were generally high for this type of radar.

The crystal detectors used in the receiver were better than those for which the set was originally designed. The nominal receiver sensitivity of −97 dbm was calculated assuming the stated noise figure for the receiver of 12.5 db and that a coherent signal can be seen 6 db below the average power of the noise.

Table 1. *Characteristics of the M-33 radar*

Characteristic	Nominal value	Measured value
Peak transmitter power	250 Kw	80 to 175 Kw
Pulse repetition frequency	1500 Hz	1465 Hz
Pulse length	75 m	75 m
Antenna gain	39 db	37 db
Antenna $\frac{1}{2}$ power beam widths	0.02 rad	—
Receiver sensitivity (MDS)	−97 dbm	−96 to −101 dbm
Frequency	8500–9600 MHz	9065 MHz

Table 2. *Characteristics of the GPG-1 radar*

Characteristic	Nominal value	Measured value
Peak transmitter power	40 Kw	22 Kw
Pulse repetition frequency	3800 Hz	3900/975 Hz
Pulse length	75 m	75 m
Antenna gain	—	31 db
Antenna ½ power beam-widths	0.057 rad	—
Receiver sensitivity (MDS)	−90 dbm	−92 dbm
Frequency	8400–9600 MHz	8780 MHz

GPG-1

The second radar, the X-band GPG-1, was planned to augment the M-33 during times of balloon tracking. The GPG-1 was also capable of tracking operations for short ranges. This radar, shown in Fig. 2*b*, was installed along the Humuula Sheep Station road at 2100 meter mean sea level elevation.

A metallic sphere calibration was made on the GPG-1 and yielded an antenna gain of 31 db. The characteristics of this radar are shown in Table 2.

Radar observations and analysis

M-33

The primary purpose of the radar facility was to provide the other investigators with information and prognostications related to the development and movement of showers imbedded in the trade winds. The radar climatological data obtained during the pursuance of these major goals of the project were somewhat limited, but certain generalizations apply to the observations made during the summer of 1965. Most of the data can be categorized into four types of radar presentations, that is, scattered showers, line showers, orographic rain, and Kona thunderstorms.

The data used for the statistical analyses were selected at random from the entire collection of radar photographs. However, the radars were operated, for the most part, only during daylight and evening hours. Therefore, any diurnal effect on the showers is not reflected in the data. Otherwise, with the exception of the first echo study, all echoes that fulfilled the requirements of a particular investigation were included in the analyses.

The analyses presented in this report consist of the relationships between echo frequency and rainfall, echo diameter frequency and range, first echo development and movement, and a discussion of typical and special cases which occurred during the program.

Echo frequency versus rainfall. A series of six one nautical mile squares were constructed on an acetate overlay as shown in Fig. 1. The squares were aligned in the direction of the prevailing trade winds. The occurrence or non-occurrence of echoes in any of the squares was tabulated at intervals of 15 minutes for nearly 212 hours of radar photographs acquired throughout the summer field program. No attempt was made to separate the data by hour of the day, intensity of echo, or synoptic conditions.

The rainfall was estimated for each of the squares from the data presented by Lavoie (1966). The results from this study are summarized in Table 3.

When the data were normalized by taking the ratio of the number of echo occurrences to the total rainfall and plotting the resulting number versus the echo occurrences, the relationship shown in Fig. 3 is obtained. The two open-circle data points which obviously do not fall on the best-fit curve were derived from the rainfall analysis over the ocean. The rainfall amounts were interpolated from the estimated rainfall gradient in a region where there were no raingages as indicated by the dashed lines in Fig. 4. However, if it is assumed that the radar data are more accurate at the lower end of the curve than the linear interpolation of rainfall data, then the rainfall over the Hilo Bay area can be derived. The results of reanalyzing the rainfall map in this region based

Table 3. *Echo frequency vs. rainfall*

Square No.	Rainfall (in.)	Echo freq. (No.)
1	15.5	167
2	16.0	233
3	15.0	150
4	13.0	99
5	9.0	67
6	7.8	72

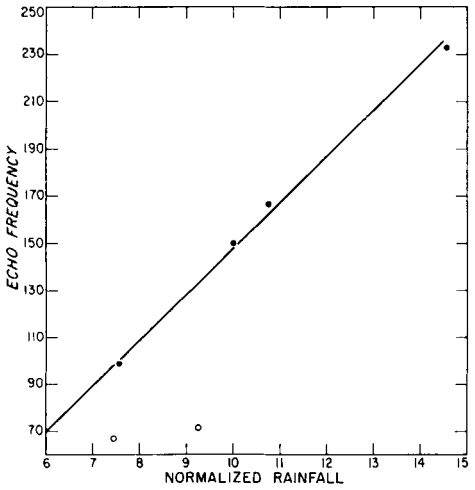

Fig. 3. The relationship between echo frequency and normalized rainfall determined from the six locations shown in Fig. 1.

upon the radar data are shown by the solid lines in Fig. 4.

The equation for the estimated best-fit line in Fig. 3 is

$$\frac{N}{R} = \frac{N+50}{20},$$

where N is the total number of echo occurrences and R is the estimated total rainfall. This equation suggests that an increase in total rainfall per echo occurrence is associated with a decrease in echo occurrences. Another way of viewing this result is that for an increase in echo occurrence the rainfall per occurrence decreases. The implication is that a long persistence echo, for example the orographic rain, producing a large echo frequency, is associated with lighter rainfall than shorter duration echoes such as showers.

No attempt was made to use rainfall and radar data acquired simultaneously for this study due to the lack of recording raingages in the area. Thus, the results are only applicable to the period under investigation and only for the radar data used. It is recommended that a future investigation be carried out using radar data and rainfall totals that are timewise correlated. The results would then be useful for the determination of rainfall totals for arbitrary periods of time so long as an adequate sample of echo occurrences is used.

Echo diameter frequency versus range. A scale was constructed from acetate consisting of a series of circles ranging from 750 to 13,500 yards in diameter in intervals of 750 yards. The radar film was scanned for isolated echoes and the diameters were noted. A total of over 2700 echoes were measured and included in this analysis. Only those echoes which were separated by at least one diameter were assumed to be isolated for the purpose of this study.

The number of echoes contained within range intervals of 10 kiloyards were tabulated and normalized by the area within the interval. Separate tabulations were made for echoes observed over land and over the ocean. No data were obtained in the interval of 0–10 kiloyards due to ground and sea clutter. Since all of the data were obtained when the radar was operated in the split-Z mode, the elevation angle of the antenna for azimuth positions between 180° and 360° entered into the area determination. The assumption was made that echoes did not penetrate the trade inversion, which according to Lavoie (1966), was at a mean altitude of 2400 meters. The result of this assumption is that the radar beam sliced through the inversion at a range of approximately 34 kiloyards over land when the split-Z mode was used. The area between 30 and 40 kiloyards was adjusted to

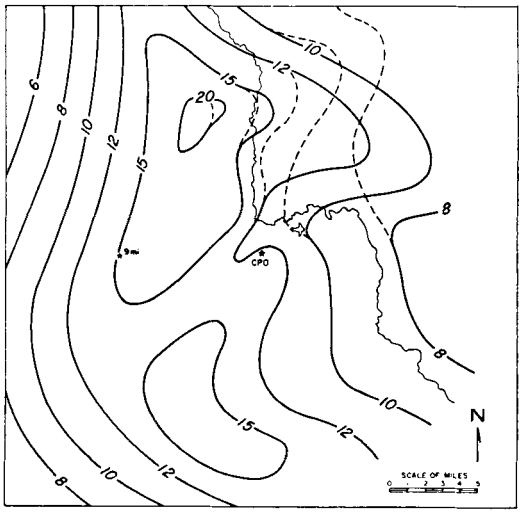

Fig. 4. The isohyetal map for the period July 11 through August 24, 1965, drawn by linear interpolation of raingage data (dashed lines) and adjusted by echo frequency (solid lines).

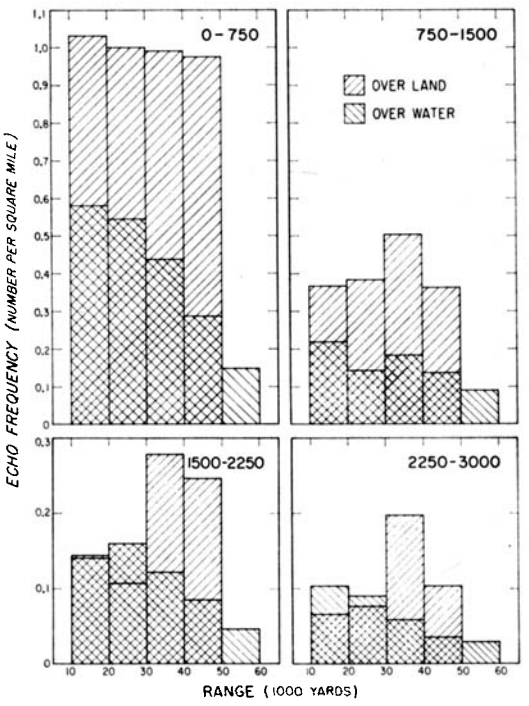

Fig. 5. Normalized echo frequency relationship to range for echoes of 0-750, 750-1500, 1500-2250, and 2250-3000 yards in diameter.

account for the antenna tilt and no over land data were tabulated beyond 40 kiloyards to the west of the radar location. However, since the antenna was at 0° elevation between 0° and 360° azimuth, all of the echo data to the 60-kiloyard range of the radar were used.

The results of the tabulations are shown in Fig. 5. The abscissa is the number of echoes per square nautical mile and the ordinate is the range interval. The dotted bars represent sea echo frequency while the open bars are land echo frequency. The four graphs represent echo diameter intervals of 0–750, 750–1500, 1500–2250, and 2250–3000 yards.

The first obvious conclusion to be drawn from the data is that the most frequent size of echo observed either over land or over the ocean is contained within the 0–750 yard diameter class interval. This class interval contains nearly twice as many echoes per square mile as larger echo diameters.

The second outstanding feature shown by these data is the decreasing frequency of over ocean echoes in all size class intervals with increasing range. This decrease cannot be accounted for by beam refraction or range effects of the radar. It simply suggests that the initial echoes appear less frequently with increasing distance from the island. The question of utmost importance to be answered then is one concerned with the influence of the island on the dynamics and thermodynamics of the sub-inversion air over the ocean in which the showers initially form.

The relative frequency of land to sea echoes shown in Fig. 5 is two to one or greater for all range intervals. This increase in number over land may be attributed to the breakup of larger echo masses or the scattering of shower lines as they move inland. Many qualitative observations of this type were noted by the radar operators during the summer.

The peak in frequency seen in Fig. 5 in the range interval of 30–40 kiloyards may, in part, be due to the assumption of the showers not penetrating the trade inversion. This assumption should be qualified in future studies to include the weakening or dissolution of the trade inversion, and also the possible increased height of larger diameter showers.

Echo initiation, movement, and dissipation. The radar film was carefully screened in order that the formation and movement of individual echoes could be studied in relation to the distance from the island and the prevailing trade winds. For the purpose of this study the echoes had to be completely isolated, and, of course, had to appear within range of the radar. As a result, very limited data were available since the majority of the showers appeared to be associated with organized lines or bands. However, even though the sample contains

Table 4. *First echo, dissipation and speed as a function of range*

Range interval (kyds)	Echo initiation	Echo dissipation	Speed at dissipation (knts)
10–20	0	10	11.9
20–30	5	18	10.8
30–40	12	11	13.4
40–50	14	7	13.4
50–60	11	4	12.6
>60	8	—	—

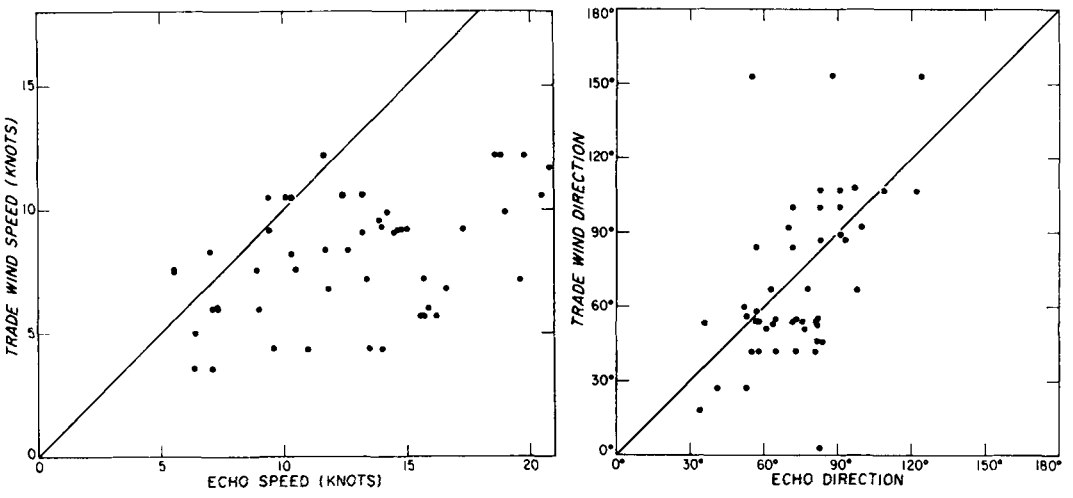

Fig. 6. The relationship between echo and trade wind speed and direction.

only 50 cases, some of the features of the data are supported by other studies.

Table 4 shows the number of first echoes and their dissipation as a function of range interval as well as their speed at the time of dissipation.

The frequency of first echoes increases with range to the 40–50 kiloyard interval and then decreases. The decrease beyond the 40–50 kiloyard range interval is substantiated by the results of the echo frequency data shown in Fig. 5. The peak frequency in echo initiation is indicative of an island effect on shower formation. In the absence of the island, the probability of first echoes would be independent of range over the ocean.

Once again a qualitative observation noted by the radar operators on numerous occasions, concerning the decrease in speed of individual echoes as they approach shore, has been substantiated by the average speeds shown in the above table. The average speed decrease is not large, but is indicative of the influence of the island on the motion of the trade wind showers.

The relationship between the echo velocity and the mean trade wind velocity through a depth comparable to the cloud was examined for the fifty isolated echoes. The correlation between the echo and trade wind speed and direction is shown in Fig. 6. The data are quite scattered and it was not deemed worthy to determine the correlation coefficient. However, it is interesting to note that the speed of the echoes is usually greater than the trade wind speed and that the echoes tend to move to the right of the wind direction. The movement of the radar echo to the right of the environmental wind is not unique to the trade wind showers as this has been observed by others in studies of mid-latitude storms (e.g., Newton & Katz, 1958). The differential in the speeds may be due to growth of the shower on the downwind side rather than to a true propagation of the individual cell. This explanation has also been invoked by other investigators to describe squall line echo behavior.

As stated previously, though, the influence of the island on the trade wind and the motion of the individual showers is not clear. The relationship between speed and direction of the wind and echo, at least in part, reflects the island effect. Additional observations of the flow about the island are necessary to clarify the relative importance of shower growth and island influence to the observed motion of trade wind showers.

Typical echo morphology and special cases. As stated before, the primary purpose of the M-33 radar was to provide the other scientists with information and prognostications on the development and movement of showers. To perform this task with some degree of success required that the radar operators observe the various echo patterns very closely and then categorize them mentally for future reference. The most typical large scale pattern of echo development and movement is shown in *a*, *b*,

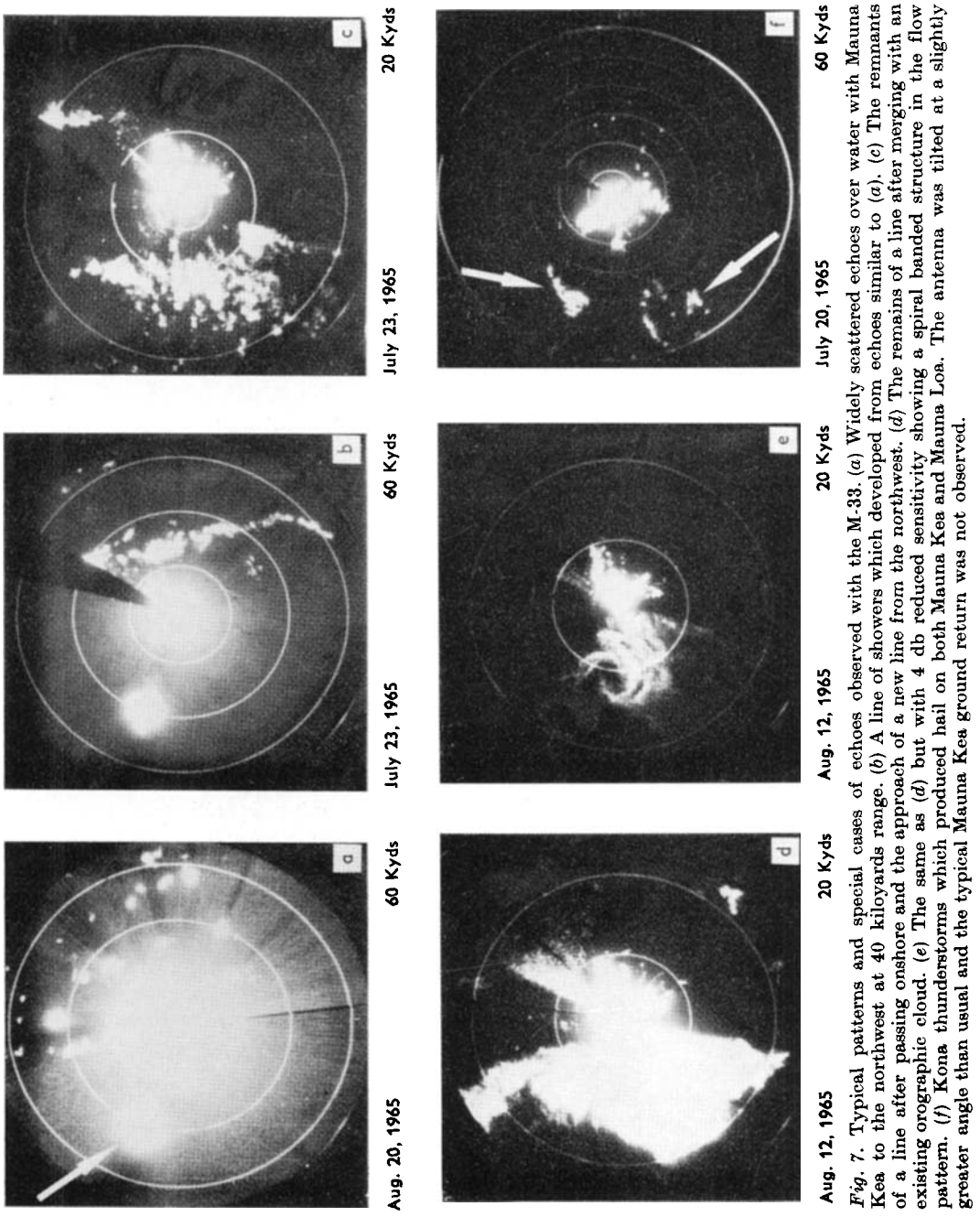

Fig. 7. Typical patterns and special cases of echoes observed with the M-33. (*a*) Widely scattered echoes over water with Mauna Kea to the northwest at 40 kiloyards range. (*b*) A line of showers which developed from echoes similar to (*a*). (*c*) The remnants of a line after passing onshore and the approach of a new line from the northwest. (*d*) The remains of a line after merging with an existing orographic cloud. (*e*) The same as (*d*) but with 4 db reduced sensitivity showing a spiral banded structure in the flow pattern. (*f*) Kona thunderstorms which produced hail on both Mauna Kea and Mauna Loa. The antenna was tilted at a slightly greater angle than usual and the typical Mauna Kea ground return was not observed.

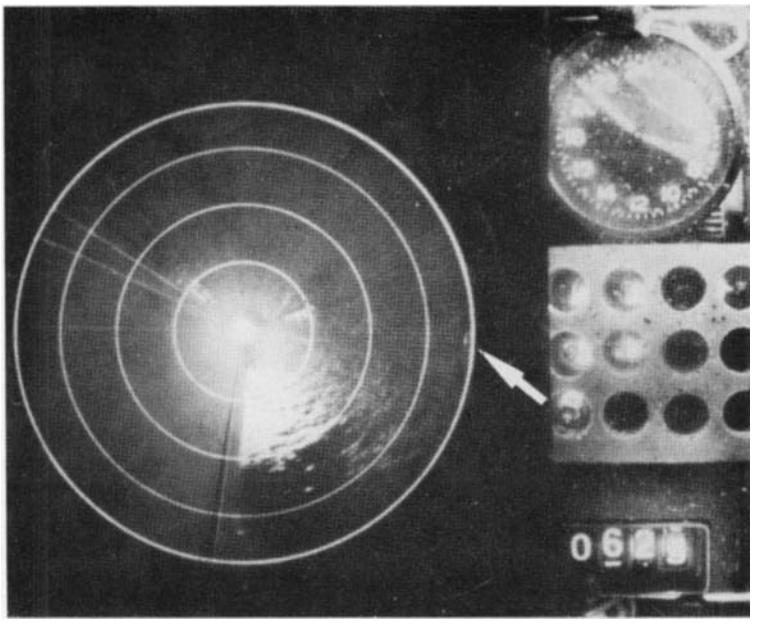

July 14, 1965

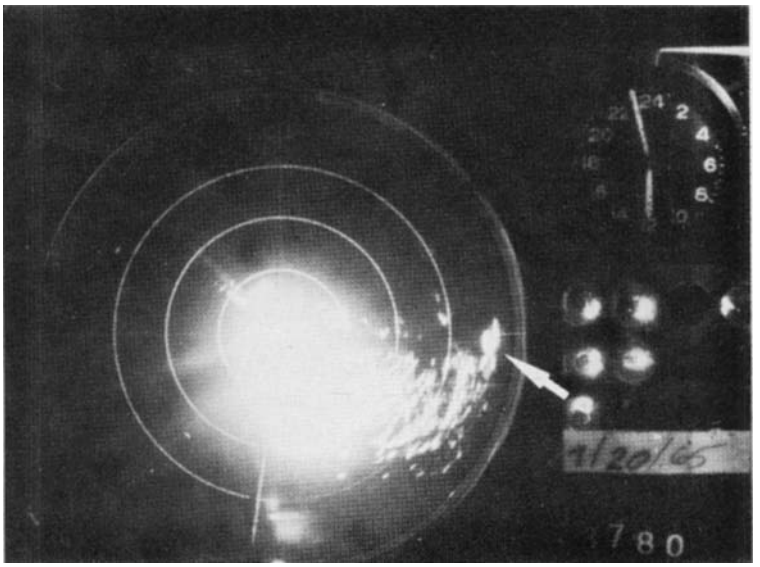

July 20, 1965

Fig. 8. Examples of differences in ground return due to the trapping gradients of the trade inversions.

and *c* of Fig. 7. During a period of approximately 30 minutes, scattered echoes appear on a previously clear scope as shown in Fig. 7*a* and continuously grow and dissipate with a lifetime of the order of 30 minutes. The next stage of development is the organization of the scattered cells into groups and bands as shown in Fig. 7*b*. There may be as many as three such bands visible at the same time with a spacing of about ten miles. Such a case is illustrated in Fig. 7*c*.

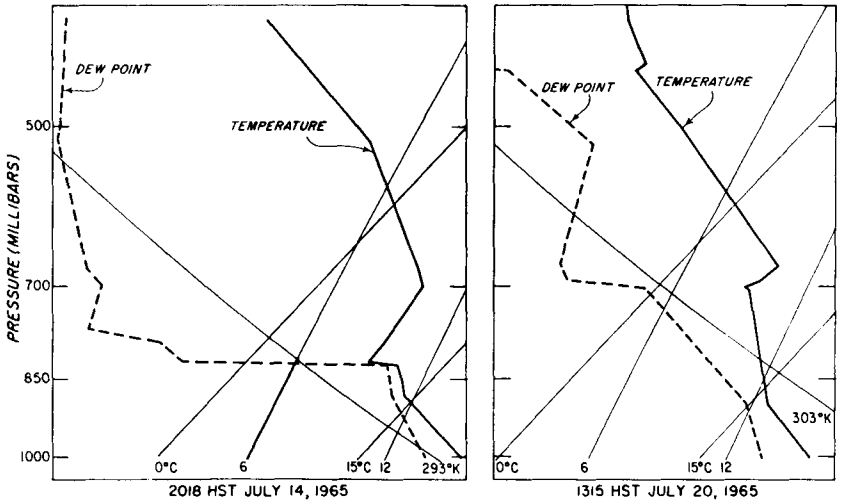

Fig. 9. Radiosonde observations at Hilo, Hawaii, on July 14 and July 20, 1965.

The bands move inland (Fig. 7*c*) and upon passing over the shore apparently begin to break up into individual cells. However, if the orographic cloud on Mauna Kea is developed at this time the cells merge with the steady rain and lose their identity.

On occasion when the orographic cloud was well developed and extended to the coastline, the shower activity was inhibited within a very short distance. Such was the situation shown in Figs. 7*d* and 7*e*. The second photo was taken approximately ten seconds after the first and at a reduced gain of 4 db. The interesting observation in this case is the apparent spiral bands noted in the reduced gain photo. This sort of presentation may be due to the lack of convective vertical motions so that the light rain associated with the echo was subject to the wind pattern generated by the interaction of the northeast trade winds and the mountain barrier on shore.

On July 20 Mauna Kea became truly the "white mountain" with a layer of what appeared to be snow, but later was found to be small hail. Several observers reported hearing thunder and some electrical activity was noted at the Mauna Loa Observatory. In the brief period of this project, this was the only day that radar echoes were observed to move from the west across the saddle between the two large mountains. The group of echoes in the southwest quadrant of Fig. 7*f* were associated with the hail. These echoes were moving to the northeast as was the echo noted to the northeast of Mauna Kea. Simultaneous with the movement of these echoes from the Kona side of the island, there were showers observed over Hilo Bay which were moving with the northeast trades toward land. During this period the sounding revealed that the trade inversion had all but disappeared and the lower layers were quite unstable. The trade winds were very light and converged with the seabreeze from the Kona area to form the hail-producing thunderstorms observed.

It must be emphasized that these were typical and special cases which were observed during the course of a two month program in 1965 and much additional data are needed before the radar climatology of the region will be realized. However, the limited cases discussed here certainly show the usefulness of radar observations in the study of tropical rainshowers and circulation patterns in the state of Hawaii.

GPG-1

The GPG-1 radar was located on Mauna Kea at 2100 meters mean sea level (see Fig. 1). This location proved to be undesirable because of the existence of a strong trapping layer which was frequently present below the radar's location. Fig. 8 shows a comparison of ground clutter for two days of operation of this radar. Calibrations on these days indicated that the

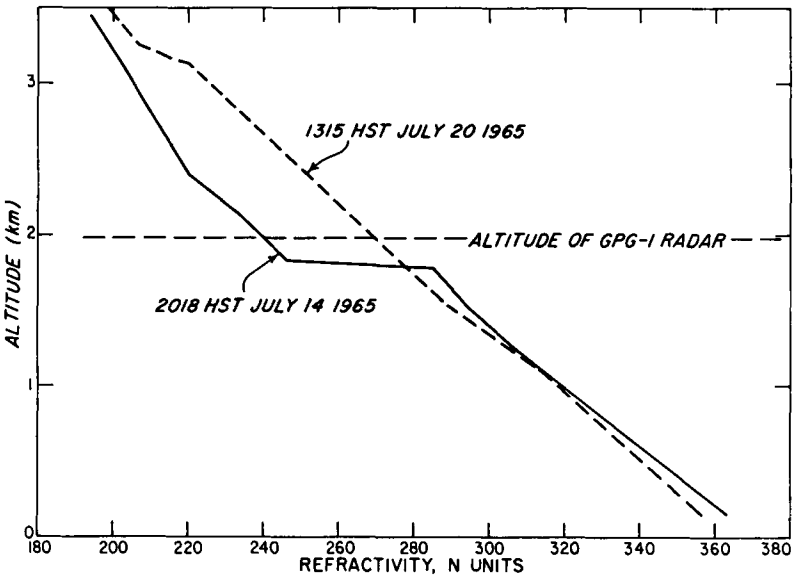

Fig. 10. Refractivity soundings derived from the radiosonde observations of July 14 and July 20, 1965.

radar was operating at about the same sensitivity. If anything, the radar was slightly more sensitive on July 14 than on July 20. In both instances the antenna was depressed 3° from the horizontal. It is immediately apparent that there is much more ground return from the eastern and southeastern sections on July 20 than on July 14. In particular, attention is directed to echoes which are due east at about 15 to 20 miles. These echoes are from oil storage tanks just east of Hilo as well as other structures around Hilo. The echoes are much weaker on July 14 (at least 10 db) and furthermore, are at a somewhat greater range than on July 20.

The explanation for this anomaly is believed to be the large gradient in refractive index associated with the trade inversion. Fig. 9 shows the Hilo soundings for July 14 and July 20. The refractivity profiles were calculated using data from these soundings with the simplified equation for refractivity given by Bean & Dutton (1966):

$$N = \frac{77 \cdot 6}{T}\left(P + \frac{4810e}{T}\right),$$

where N is the refractivity, T is the temperature in degrees kelvin, P is the pressure in millibars and e is the vapor pressure in millibars. The refractivity soundings are shown in Fig. 10. The analysis shows that on July 14 the inversion is below the radar and on July 20 the inversion, if it exists at all, is well above the radar. The gradient on July 14 was 780 N units per kilometer. Further radiosonde analysis has shown that more than one half of the time, refractivity gradients in excess of 150 N units per kilometer were in existence below the radar height of the GPG-1 for the period July 11 through July 31.

According to Bean & Dutton, a gradient in excess of 150 N units per kilometer produces trapping. Thus it is not surprising to note such large differences in ground return for a gradient of 780 N units per kilometer.

This large uncertainty in the validity of data obtained from this location dictated the cessation of operation of this radar. Consequently, the GPG-1 was dismantled and removed late in July and attention was focused on the M-33 at the Cloud Physics Observatory.

Summary

Two X-band radars, a tracking M-33 and a GPG-1, were used extensively during the period July 11 through August 24, 1965, to obtain data on trade wind showers near the island of

Hawaii in support of an international cloud physics program. The M-33 radar proved to be a valuable tool for the study of trade wind showers in Hawaii. The relationship between echo frequency and rainfall was exceptionally good for the period of the field program.

The frequency of echoes of a given diameter as a function of range is indicative of the climatology of shower evolution. These results coupled with the dependence of echo movement on the trade winds provided limited quantitative information on the development, size, and movement of trade wind showers.

The GPG-1 was operated for a brief period of time at the 2100 meters elevation on the windward slopes of Mauna Kea. Due to unfavorable atmospheric conditions at this location, the radar was returned to the CPO and full effort was devoted to the operation and maintenance of the M-33.

Acknowledgments

Special thanks are due Dr. E. J. Workman and Mr. R. L. Lavoie of the University of Hawaii, who provided solutions to the many logistical problems encountered during the field project. Our thanks go to Mr. J. Tefft of the National Center for Atmospheric Research for the modification and installation of the M-33 tracking radar at the Cloud Physics Observatory. This work was supported by National Science Foundation grant NSF GP-194.

REFERENCES

Bean, B. R. & E. J. Dutton, 1966. *Radio Meteorology*, NBS Monograph 92. U.S. Government Printing Office, Washington, 435 pp.

Lavoie, R. L. 1966. Background data for the warm rain project, *Tellus 19*, 348–353.

Newton, C. W. & S. Katz, 1958. Movement of large convective rainstorms in relation to winds aloft. *Bull. Am. Meteorol. Soc. 39*, 129–136.

РАДИОЛОКАЦИОННЫЙ АНАЛИЗ ТЕПЛЫХ ЛИВНЕЙ

Два радиолокатора со скрещенными лучами M-33 и GPG-1 работали стандартным образом на о. Гавайи в период с 11 июля по 28 августа 1965 г. Радиолокатор M-33 находился на территории Обсерватории физики облаков в отделении Хило Гавайского университета. Данные, полученные фотографированием ИКО, были использованы для определения предварительных климатологических параметров, связанных с пассатными ливнями.

Проверялось соотношение между частотой эхо и полным количеством осадков и было найдено, что оно выполняется очень хорошо. Такой анализ полезен для определения количества осадков над сушей и океаном вблизи Гавайских о-вов, где мала плотность сети осадкомеров.

Частота эхо данного диаметра как функция расстояния была протабулирована отдельно для наблюдений над сушей и над водой. Из этих данных следует, что частота эхо над единицей площади над сушей больше, чем над водой. Это связывается с разрушением регулярных линий или полос ливней по мере их продвижения внутрь суши. В дополнение, существует заметное уменьшение частоты эхо с расстоянием. Это уменьшение не может быть объяснено ослаблением отраженного сигнала о расстоянием или атмосферной рефракцией.

Изучалась связь между движениями эхо и пассатами. Результаты показывают, что радиолокационные эхо имеют тенденцию двигается вправо от направления ветра со скоростями, несколько большими, чем скорости ветра в данном месте.

Представлено несколько примеров фотографии ИКО, иллюстритующих типичные распределения отраженных сигналов. Показаны также фотографии сигналов от мезосистемы и эхо, связанных с грозой.

Радиолокатор GPG-1 размещался на высоте 2100 м на подветренном склоне вулкана Мауна Кеа. Очень мало полезных данных было получено с его помощью, поскольку в этом месте существуют неблагоприятные (для дождей) градиенты, связанные с инверсией в пассатах. Дается пример, для которого путь распространения луча был увеличен, а чувствительность понижена благодаря существованию градиента показателя преломления. Это место было вскоре оставлено для большей концентрации усилий в работе с локатором M-33.